PARAMETRIC HARMONIC BALANCE*

Yngve Thodesen
Department of Telecommunications
Norwegian University of Science and Technology
7034 Trondheim, Norway

Ken Kundert
Cadence Design Systems
San Jose, California 95134

Abstract

Harmonic balance has established itself as an important technique for simulating high frequency circuits. However, this simulator struggles on strongly nonlinear circuits, particularly if there are several input signals at different frequencies.

An important observation is that multi-tone nonlinear circuits usually react in a strongly nonlinear fashion in response to one signal, but in near-linear fashion in response to the others. In this paper we present an extension of harmonic balance that exploits these properties to reduce the time and memory required to perform accurate circuit-level frequency-domain simulation of mixers.

1 Introduction

The most popular method for simulating high frequency circuits is harmonic balance (HB) [kundert90]. However, using HB to simulate communication circuits that have two or more input tones will typically be a slow and memory-consuming process. An important observation is that these circuits typically respond in a strongly nonlinear fashion to only one input signal (the *large signal*). Commercial harmonic balance simulators such as HP's Microwave Nonlinear Simulator (MNS) provide analyses where they linearize the harmonic balance equations of the circuit about the solution that results when only the large signal is applied [held78, kerr79] and apply the small signal to the resulting linearized periodically time-varying circuit. However, this method gives no spurious frequencies of the small signal.

This paper proposes a new harmonic balance

method for simulating the large / small signal problem that exploits its nature — strongly nonlinear for the large signal and weakly nonlinear for the small signal. The technique, in this paper called parametric harmonic balance (PHB), is based on partitioning the simulation into two stages. The first stage solves a strongly nonlinear problem and the second solves a weakly nonlinear perturbation of the first. As a result, PHB becomes much faster and uses much less memory than HB on circuits such as mixers. Therefore it is possible to simulate those circuits at an ordinary workstation, with enough harmonics to assure accurate results.

2 The Method

An electronic circuit constructed of nonlinear resistors, nonlinear capacitors, and lumped and distributed linear components may be described in the frequency domain with the following equation [kundert90]

$$H(V) = YV + \Omega Q(V) + I(V) - U = 0 \qquad (1)$$

where $I(V)$ is the vector of nonlinear resistor node currents, $Q(V)$ is the vector of nonlinear capacitor charges, and Y is the phasor representation of the node admittance matrix for the linear components (lumped and distributed). Equation (1) is most effectively solved by using the Newton-Raphson algorithm [ortega70].

$$J_H(V^{(j)})(V^{(j+1)} - V^{(j)}) = -H(V^{(j)}) \qquad (2)$$

In this paper we are focusing on circuits with the special input $U = U_L + U_S$. The circuit will respond with $V = V_L + V_S$. Usually, U_L represents the local oscillator signal, which is large in the sense that the circuit responds in a strongly nonlinear fashion — V_L. U_S represents the input signal, which is small in the sense that the circuit responds in a weakly nonlinear fashion — V_S.

2.1 Stage 1

In stage 1 we set $U_S = 0$ and force the circuit with $U = U_L$. The circuit will respond with $V = V_L$. For simplicity, we will assume that U_L, and hence V_L, is periodic. To make the problem tractable, we need to bound the number of harmonics by assuming energy in harmonics greater than $2M - 1$ is negligible. Thus, $2M$ frequencies are included in the first stage. Using double the number harmonics in the first stage gives less aliasing error in the DFT and a better Jacobian (better convergence) in stage 2. We then have $Y \in \mathcal{C}^{2NM \times 2NM}$, $Q \in \mathcal{C}^{2NM}$, $I \in \mathcal{C}^{2NM}$, $U_L \in \mathcal{C}^{2NM}$ and $V_L \in \mathcal{C}^{2NM}$. N is the number of nodes in the circuit.

$J_1 \in \mathcal{C}^{2NM \times 2NM}$ given by (3) is the Jacobian in stage 1.

$$J_1(V_L) = Y + \Omega \frac{\partial Q(V_L)}{\partial V} + \frac{\partial I(V_L)}{\partial V} \qquad (3)$$

2.2 Stage 2

Two small tones with $M_S - 1$ harmonics used for each, give $R = M_S \cdot (M_S - 1) + 1$ small tone frequencies when the diamond truncation is used (see figure 1). We write $U_S = [\; U_1 \quad U_2 \quad \ldots \quad U_R \;]^T$ and $V_S = [\; V_1 \quad V_2 \quad \ldots \quad V_R \;]^T$, where U_1, $V_1 \in \mathcal{C}^{2NM}$ and U_r, $V_r \in \mathcal{C}^{N(2M-1)}$, $r = 2, 3, \ldots, R$. V_L is already known when stage 2 starts, and therefore U_L and V_L may be included in the circuit.

$$\tilde{Q}_r(V_S) =$$

$$\tilde{Q}_r \left(\begin{bmatrix} V_1 \\ V_2 \\ \vdots \\ V_{R_F} \end{bmatrix} \right) = Q_r \left(\begin{bmatrix} V_L + V_1 \\ V_2 \\ \vdots \\ V_{R_F} \end{bmatrix} \right) - Q_r \left(\begin{bmatrix} V_L \\ 0 \\ \vdots \\ 0 \end{bmatrix} \right)$$

$$(4)$$

and

$$\tilde{Q}(V_S) = [\; \tilde{Q}_1(V_S) \quad \tilde{Q}_2(V_S) \quad \ldots \quad \tilde{Q}_R(V_S) \;]^T \qquad (5)$$

The same is done to get $\tilde{I}(V_S)$. This change causes the circuit to become a *parametric circuit* [locherer82].

Equation (6) describes the problem in stage 2.

$$H(V_S) = [\; H_1(V_S) \quad H_2(V_S) \quad \ldots \quad H_R(V_S) \;]^T \qquad (6)$$

where

$$H_r(V_S) = Y_r V_r + \Omega_r \tilde{Q}_r(V_S) + \tilde{I}_r(V_S) - U_r = 0 \\ r = 1, 2, \ldots, R$$

$$(7)$$

$J_2 \in \mathcal{C}^{NK \times NK}$ given by (8) is the Jacobian in stage 2. $K = (R - 1) \cdot (2M - 1) + 2M$.

$$J_2(V_S) = [J_{r_1 r_2}(V_S)], \quad r_1, r_2 = 1, 2, \ldots, R$$

where

$$J_{r_1 r_2}(V_S) =$$

$$\begin{cases} Y_{r_1} + \Omega_{r_1} \dfrac{\partial \tilde{Q}_{r_1}(V_S)}{\partial V_{r_2}} + \dfrac{\partial \tilde{I}_{r_1}(V_S)}{\partial V_{r_2}}, & r_1 = r_2 \\[3mm] \Omega_{r_1} \dfrac{\partial \tilde{Q}_{r_1}(V_S)}{\partial V_{r_2}} + \dfrac{\partial \tilde{I}_{r_1}(V_S)}{\partial V_{r_2}}, & r_1 \neq r_2 \end{cases}$$

$$(8)$$

To accelerate the Newton-Raphson iteration we make two approximations to the Jacobian J_2. First, we apply Samanskii's method [ortega70]. Second, we apply nonlinear block Gauss-Seidel relaxation [ortega70]. The motivation for doing these simplifications, is the assumption that the circuit is weakly nonlinear for the small signal. This implies that the numbers in $J_{r_1 r_2}(V_S)$, $r_1 \neq r_2$ are small compared to the numbers in $J_{r_1 r_2}(V_S)$, $r_1 = r_2$. Thus the iterative method in stage 2 may be described by (9).

$$\text{diag} \left(J_{11}(V_S^{(0)}), J_{22}(V_S^{(0)}), \ldots, J_{RR}(V_S^{(0)}) \right) \cdot$$

$$(V_S^{(j+1)} - V_S^{(j)}) = -H(V_S^{(j)})$$

$$j = 0, 1, 2, \ldots \qquad (9)$$

with $J_{11} \in \mathcal{C}^{2NM \times 2NM}$ and $J_{rr} \in \mathcal{C}^{N(2M-1) \times N(2M-1)}$ with $r = 2, 3, \ldots, R$.

Nonlinear Gauss-Seidel relaxation [ortega70] is applied to solve (9), which gives the algorithm described by (10).

$$J_{rr}(V_S^{(0)})(V_r^{(j+1)} - V_r^{(j)}) =$$

$$-H_r([\; V_1^{(j+1)} \quad \ldots \quad V_{r-1}^{(j+1)} \quad V_r^{(j)} \quad \ldots \quad V_R^{(j)} \;]^T)$$

$$r = 1, 2, \ldots, R \qquad (10)$$

with $j = 0, 1, 2, \ldots$ and

$$J_{rr}(V_S^{(0)}) = Y_r + \Omega_r \frac{\partial \tilde{Q}_r(V_S^{(0)})}{\partial V_r} + \frac{\partial \tilde{I}_r(V_S^{(0)})}{\partial V_r} \qquad (11)$$

For $r = 1$, (10) must be the same equation as the one used in stage 1, to improve convergence in stage 2.

An ordinary DFT is used in the transformation between frequency and time domain. To make this possible *the false frequency approach* [kundert90] is used, optimized for this large / small signal problem (see figure 1).
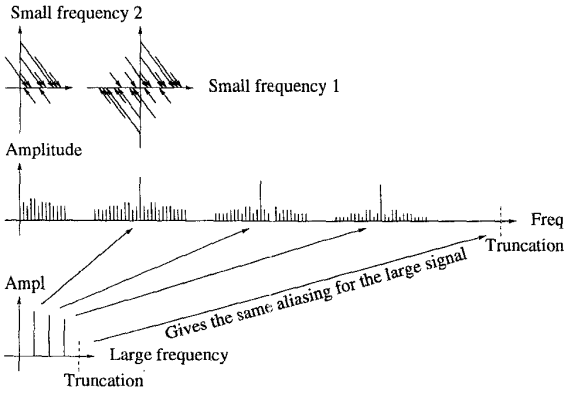
Figure 1: Preparing the vector before applying the DFT. This approach maintains the aliasing pattern of stage 1, which improves convergence in stage 2.

3 Computational Costs

The memory needed to store the Jacobian in HB is order $(MR)^2 N$, while that of PHB is order $M^2 RN$. The memory use is roughly R times higher in HB.

The operations needed for factoring the Jacobian in HB is order $(MR)^3 NJ$ (J is the number of times the Jacobian has to be loaded and factored), while that of PHB is order $M^3 RN$. Even if Samanskii's method is used to speed up HB, the cost to factor the Jacobian is still roughly R^2 times more expensive.

4 Results

In this section we apply PHB to the following four mixers.

1. Double balanced image rejection diode mixer with passive baluns. Lumped element circuit. Contains 8 diodes, 35 resistors, 33 capacitors and 29 inductors. $M = 16$, $R = 13$ and $N = 88$.

2. Double balanced image rejection diode mixer with passive baluns. Distributed elements in the microwave part. Contains 8 diodes, 19 resistors, 14 capacitors, 12 inductors and 13 transmission lines. $M = 16$, $R = 13$ and $N = 80$.

3. Double balanced image rejection resistive FET mixer with active high frequency baluns (large signal and mixed signal) and passive low frequency baluns (moderate signal). Contains 17

Circuit	1	2	3	4
Passive components	97 lu	45 lu + 13 di	70 lu	52 lu
Active components	8 dio	8 dio	17 FETs	21 FETs
N	88	80	98	105
M	16	16	8	8
R	13	13	13	13
Time (Stage 1)	1m 51s	2m 46s	1m 31s	1m 38s
Time (Stage 2)	46m 36s	50m 20s	59m	36m 36s
Time (HB)	2d 3h	3d 1h	1d 7h	9h
Mem [Mb] (PHB)	8.3	7.5	2.2	2.3
Mem [Mb] (HB)	108	97.5	28.6	29.9

Table 1: Simulation times and memory use for PHB on four mixers. The time-use for HB is estimated. lu = lumped, di = distributed, dio = diodes, d = days, h = hours, m = minutes and s = seconds.

transistors, 28 resistors, 25 capacitors, 17 inductors. $M = 8$, $R = 13$ and $N = 98$.

4. Unbalanced distributed FET mixer with active combiner for large signal and moderate signal. Contains 21 transistors, 8 resistors, 4 capacitors and 40 inductors. $M = 8$, $R = 13$ and $N = 105$.

In all test circuits we have used the same frequencies: $f_L = 6$ GHz, $f_{S1} = 69$ MHz, $f_{S2} = 71$ MHz. 3 harmonics used for each small signal, give $R = 13$. The simulating times in table 1 is for one point (Circ. 1, 2, 3: -6.48 dBm and 4: -42 dBm) in figure 2 and figure 3. All simulations are done on a SUN IPC (Sparc 1) workstation.

5 Conclusion

PHB has proved to have a strong convergence, even though the Jacobian is simplified for making the method nearly R^2 times faster than HB. The simulation-times were not compared in practice because HB needs nearly R times the memory to run. Since no computer was available that had sufficient memory to run standard harmonic balance, its simulation-times had to be estimated.
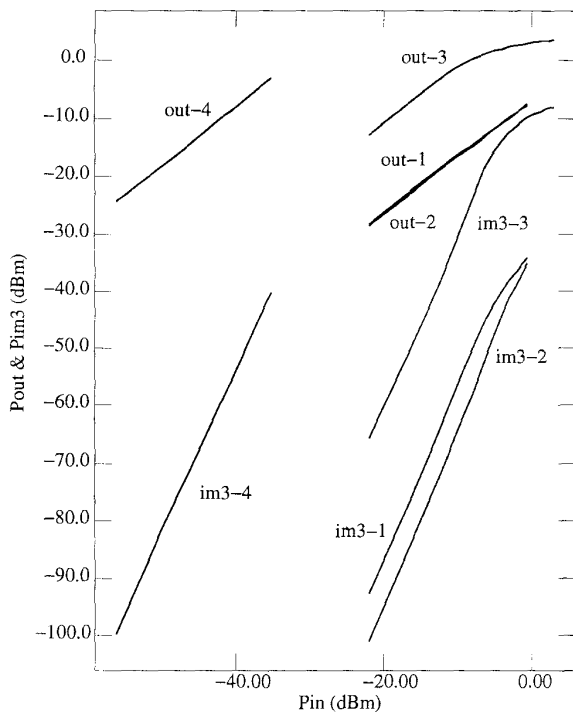
Figure 2: Output from four mixers. Pin is the small signal input.
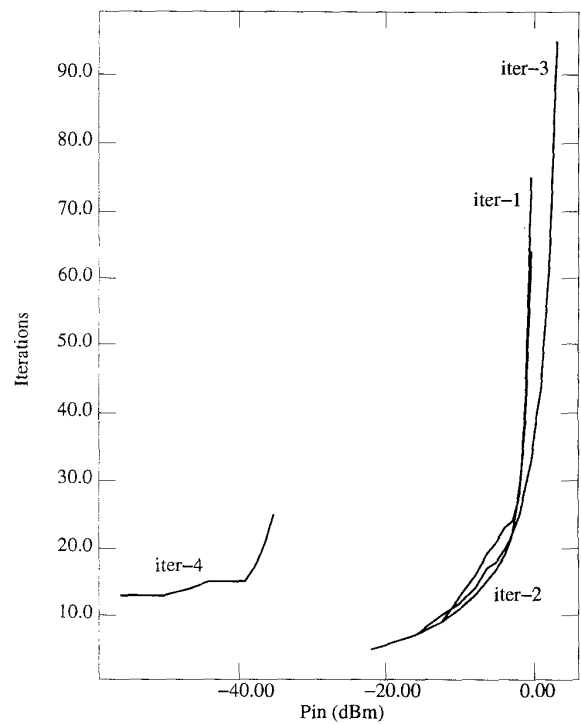
Figure 3: Iterations involved in stage 2. Pin is the small signal input.

References

[held78]   D. N. Held and A. R. Kerr. Conversion loss and noise of microwave and millimeter-wave mixers. *IEEE Transactions on Microwave Theory and Techniques*, vol. MTT-26, no. 2, February 1978, pp. 49-61.

[kerr79]   A. R. Kerr. Noise and loss in balanced and subharmonically pumped mixers. *IEEE Transactions on Microwave Theory and Techniques*, vol. MTT-27, no. 12, December 1979, pp. 938-950.

[kundert90] K. S. Kundert, Jacob K. White and Alberto Sangiovanni-Vincentelli. *Steady-State Methods for Simulating Analog and Microwave Circuits*. Kluwer Academic Publishers, 1990.

[locherer82] K. H. Locherer and C. D. Brandt. *Parametric Electronics*. Springer-Verlag Berlin Heidelberg New York, 1982.

[ortega70]   J. M. Ortega and W. C. Rheinboldt. *Iterative Solution of Nonlinear Equations in Several Variables*. Academic Press, 1970.